catalysts

MDPI

Article

Highly Photoactive Titanium Dioxide Supported Platinum Catalyst: Synthesis Using Cleaner Ultrasound Approach

Shital B. Potdar [1], Chao-Ming Huang [2,*], BVS Praveen [3], Sivakumar Manickam [4] and Shirish H. Sonawane [1,*]

[1] Department of Chemical Engineering, National Institute of Technology Warangal, Warangal 506004, Telangana, India; shital@student.nitw.ac.in
[2] Green Energy Technology Research Center, Department of Materials Engineering, Kun Shan University, Tainan 710, Taiwan
[3] Department of Chemical Engineering, BV Raju Institute of Technology, Narsapur 502313, Telangana, India; praveen.bvs@bvrit.ac.in
[4] Petroleum and Chemical Engineering, Faculty of Engineering, Universiti Teknologi Brunei, Bandar Seri Begawan BE1410, Brunei; manickam.sivakumar@utb.edu.bn
* Correspondence: charming@mail.ksu.edu.tw (C.-M.H.); shirish@nitw.ac.in (S.H.S.)

Abstract: Catalysts increase reaction rates; however, the surface area to volume ratio of catalysts has a vital role in catalytic activity. The noble metals such as platinum (Pt) and gold (Au) are expensive; despite this, they have proven their existence in catalysis, motivating the synthesis of supported metal catalysts. Metal catalysts need to be highly dispersed onto the support. In this investigation, an ultrasound approach has been attempted to synthesise highly photoactive titanium dioxide (TiO_2) nanoparticles by the hydrolysis of titanium tetraisopropoxide in an acetone/methanol mixture. To enhance its photocatalytic activity, TiO_2 was doped with Pt. The synthesised photocatalyst was characterised by techniques such as particle size analysis (PSA), XRD, FE-SEM, TEM, and EDX. The enhancement in the surface characteristics of Pt-doped TiO_2 compared with bare TiO_2 support was confirmed with Brunauer–Emmett–Teller (BET) analysis. The enhanced surface area and uniformity in particle size distribution at the nanoscale level were due to the effects of ultrasonic irradiation. The obtained results corroborated the size and composition of the synthesised catalysts. The size of the catalysts is in the nanometre range, and good dispersion of Pt catalysts over the TiO_2 support was observed. The UV-Visible spectroscopy analysis was performed to study the optical properties of the synthesised TiO_2 and Pt/TiO_2 photocatalysts. An increase in the absorbance was noted when Pt was added to TiO_2, which is due to the decrease in the band gap energy.

Keywords: photocatalyst; ultrasound; titanium dioxide; platinum; photocatalytic activity; nano

Citation: Potdar, S.B.; Huang, C.-M.; Praveen, B.; Manickam, S.; Sonawane, S.H. Highly Photoactive Titanium Dioxide Supported Platinum Catalyst: Synthesis Using Cleaner Ultrasound Approach. *Catalysts* **2022**, *12*, 78. https://doi.org/10.3390/catal12010078

Academic Editor: Didier Robert

Received: 14 December 2021
Accepted: 29 December 2021
Published: 11 January 2022

1. Introduction

Photocatalysis is a technique that harnesses the available abundant solar energy; in it, a photon drives a chemical reaction in the presence of a catalyst. The process is eco-friendly and non-hazardous [1] and is one of the most preferred methods for purifying the pollutants in the atmosphere and aquatic systems [2]. Titanium dioxide (TiO_2) is a widely used photocatalyst, considering its good catalytic activity, high stability, low cost, and suitable band gap energy [3,4], and hence is beneficial in many applications such as oxidation reactions [5], solar cells [6], hydrogen production [7], water treatment [8,9], and degradation of pollutants [10].

Various dopants are impregnated into TiO_2 to extend the sensitivity in the visible spectral range [11]. This process also helps in minimising the surface charge transfer [12]. The metal catalysts doping/impregnation concept has been gaining more importance recently. Here, the primary catalyst is dispersed on a suitable support, obtaining stable nanoparticles (NPs) and reducing costly metal utilisation [13]. Metals used include niobium [6], copper and nickel [7], iron [8], cobalt [12] silver [14], chromium [15], molybdenum [16],

vanadium [17], silver [18], ruthenium, and platinum [19]. The Schottky barrier formed between TiO_2 and metal dopant acts as a source of electron traps or recombination sites to increase the efficiency of TiO_2 [20]. Among the above, platinum (Pt) doped TiO_2 gives better photocatalytic activity, extending the light absorption to the visible band [21,22]. There are broad-spectrum applications of Pt-doped TiO_2, especially in the degradation of dye [23,24], decomposition of phenol [11], and solar energy utilisation [25]. Even though Pt is expensive and has limited commercial usage, it can be compensated for by immobilising suitable supports like TiO_2 [25]. Various methods are available for doped TiO_2 syntheses, such as sol-gel [26,27], suspension impregnation [28], solid-state reaction [29], sonochemical synthesis [19], and hydrothermal method [30] to manipulate the NPs' shape, size, and other physical properties. In the sonochemical synthesis, the ultrasound-induced chemical effect is attributed to the temperature rise caused by alternating compression and rarefaction cycles of acoustic cavitation. The hot spots are formed due to the rapid formation of the bubbles, their growth and collapse in the liquid media resulting in the metal ions reduction to metals and metal oxides. The sonochemical technique provides local temperatures of more than 5000 K, pressures more than 20 MPa, and a very high cooling rate during cavitation bubble collapse, causing special and unique properties for NPs [31].

Very little literature is available for the Pt doped TiO_2 NPs synthesis using the sonochemical method. Teoh et al. [32] reported a one-step Pt/TiO_2 synthesis using a flame spray pyrolysis reactor with controlled crystallite size and surface area. The synthesised particles exhibited rutile and anatase phases. Shanmugam and Gedaken [33] reported the synthesis of Pt NPs on mesoporous anatase TiO_2 using the ultrasound-assisted polyol reduction method. The obtained particles were in the range of 100 to 200 nm and were employed for the oxygen reduction reaction. Neppolian et al. [34] reported synthesising Pt, graphene oxide (GO), and TiO_2 photocatalyst. Initially, TiO_2 particles were synthesised using the pH swing method. Later, the ultrasound-assisted hydrothermal method was employed to obtain GO-TiO_2 NPs. Graphene oxide was initially dispersed in a water and ethanol solution mixture and sonicated for 2 h, and the required amount of TiO_2 was then added. To this known wt% of Pt was doped using the photochemical reduction method.

Bedolla et al. [35] synthesised Pt/TiO_2 utilising acid-treated TiO_2 dispersed in isopropyl alcohol using a sonicator probe. At the same time, Pt precursor (H_2PtCl_6) was sonicated in an ultrasonic bath. The two solutions were mixed, to which sodium borohydride reducing agent was added and subjected to sonication. A black precipitate was formed after sonicating for 20 min. The surface area of the synthesised catalyst from BET analysis is 193 m^2/g. The synthesised particles were used as catalysts in direct methanol fuel cell applications. Abdulrazzak et al. [36] reported the synthesis of Pt-impregnated TiO_2 coated on carbon nanotubes using the sonochemical hydration-dehydration method. TiO_2 particles were uniformly distributed on the carbon NPs surface, then coated by Pt NPs. In all the reports, the particle sizes of Pt/TiO_2 synthesised by ultrasound methods are more than 50 nm. By contrast, in this study, the synthesised particles were with the size of <20 nm.

The available research work done earlier showed that the size of Pt/TiO_2 NPs is in the range of 50 nm or more. This study aims to synthesise anatase phase Pt-doped TiO_2 NPs with a particle size less than 20 nm using an ultrasound approach. The synthesised particles are characterised using transmission electron microscopy and particle size analyser to study the particle size, X-ray diffraction to study the phase structure, BET analysis to study the pore size, and EDS to study the composition. The data obtained are compared with the available literature as and when required.

2. Results and Discussion

2.1. Photocatalytic Activity of TiO_2 and Pt/TiO_2

The UV Visible spectroscopy analysis was performed to study the optical properties of the synthesised TiO_2 and Pt/TiO_2 photocatalysts. Figure 1 shows the UV-Vis spectroscopy of TiO_2 NPs and Pt-doped TiO_2 NPs. The spectra were obtained in the wavelength range

of 200 to 1100 nm. No changes in the spectral absorbance were observed beyond the wavelength of 400 nm. From Figure 1, strong absorption was observed in the wavelength range below 400 nm. This is due to the band gap absorption of TiO_2. An increase in the absorbance has been observed when Pt is added to TiO_2. This is attributed to the decrease in the band gap energy [37]. The band gap energy calculated from the UV spectrum of TiO_2 is 3.2 eV [38]. In comparison, the band gap energy for the Pt/TiO_2 decreases to 2.89 eV when TiO_2 is doped with platinum. The mechanism for the photocatalytic activity with a decrease in band gap is shown in Figure 2.

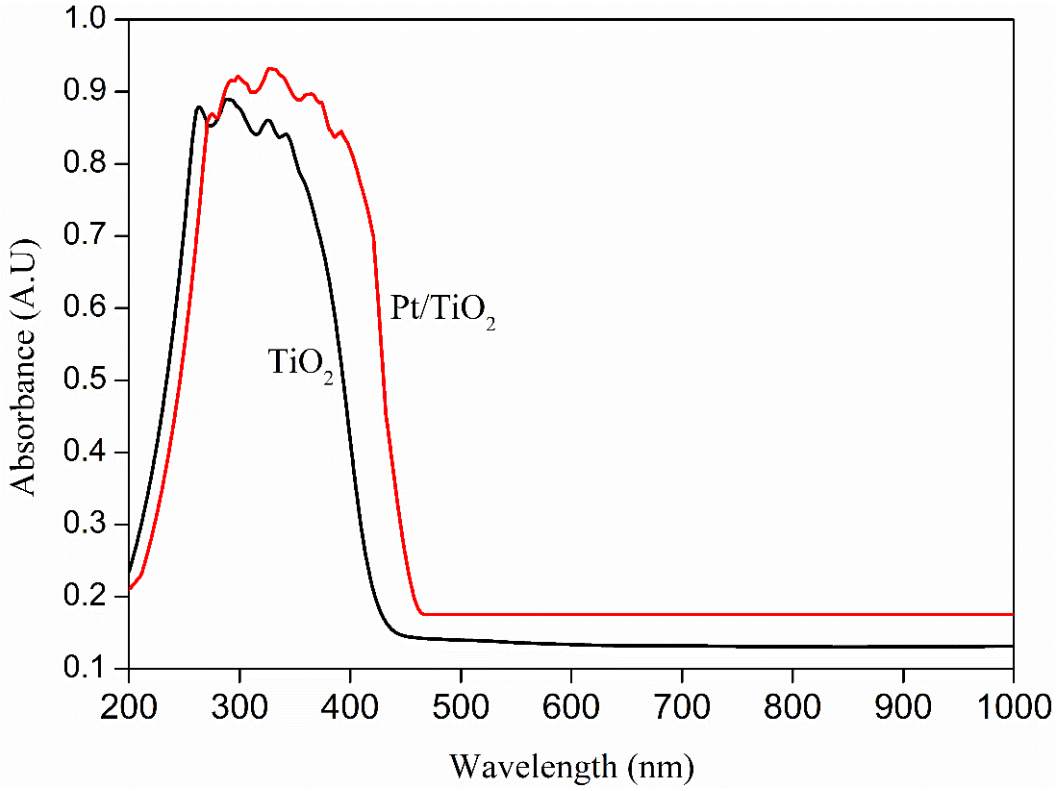

Figure 1. UV-Visible spectra of TiO_2 and Pt/TiO_2.

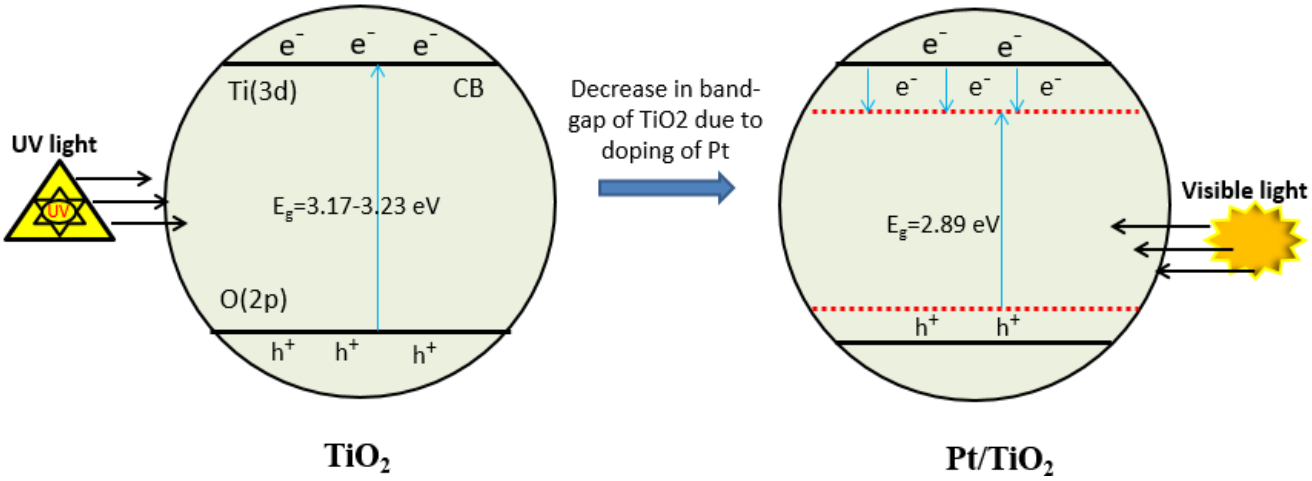

Figure 2. Mechanism for the contraction in the band gap of TiO_2 due to doping with noble metal Pt.

2.2. Mechanism of Doping of Noble Metal Pt on the Surface of TiO_2

TiO_2 NPs function better under UV rays considering their large band gap [39]. However, they suffer from the fast recombination of excited electrons and holes [40]. Hence,

TiO_2 NPs are modified to be better utilised in the visible range. Figure 2 illustrates the mechanism of the band gap decrease of TiO_2 because of the impregnation of Pt. The recombination of the electron-hole pair was reported to be retarded significantly due to the deposition of noble metals such as Au and Pt on TiO_2. This phenomenon assists in extending the wavelength response to the visible range [41–44].

2.3. Particle Size Analysis of TiO_2 Support and TiO_2 Supported Pt Photocatalyst

Figure 3 shows the particle size obtained from dynamic light scattering analysis for TiO_2 and TiO_2-supported Pt photocatalyst. Both show a single peak corresponding to uniform particle size distribution. The size distribution of TiO_2 support is observed to be between 15 nm and 120 nm. The average particle size of TiO_2 particles is about 37 nm, whereas, in the case of TiO_2-supported Pt catalysts, it increased slightly to 43 nm. The particle size analysis facilitates analysing the distribution of the synthesised photocatalyst. However, it failed to give the crystallinity and morphology of the obtained particles. Hence XRD and TEM analyses were employed. The size of the synthesised support and photocatalyst in the nano range (<50 nm) can be attributed to turbulence and intense shear effects of the ultrasound-induced cavitation.

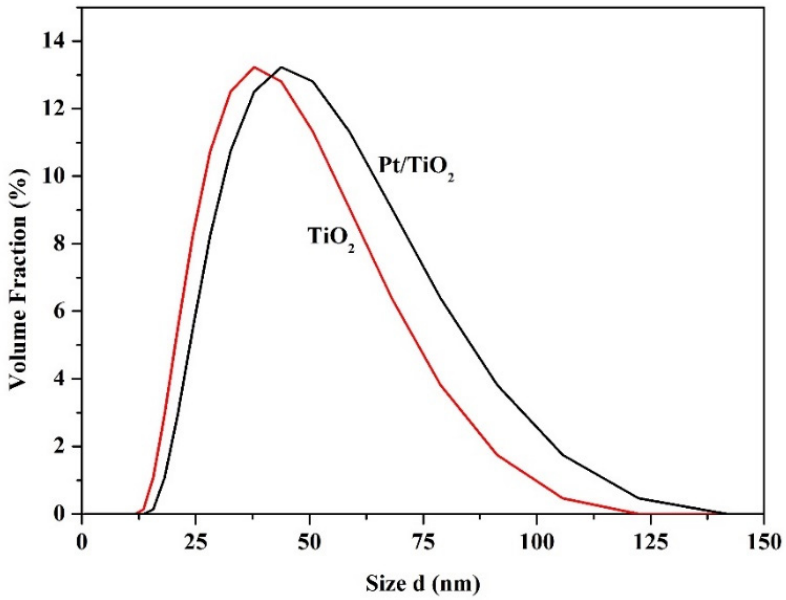

Figure 3. PSA of TiO_2 and TiO_2 supported Pt catalyst.

2.4. XRD and BET Analysis of TiO_2 Support and TiO_2 Supported Pt Photocatalyst

Figure 4 depicts the XRD spectra of pure TiO_2 and Pt-doped TiO_2 NPs, and the peaks at 2θ values of 25.3, 37.85, 48.01, 55.03, 62.66, and 70.06 for TiO_2 and Pt/TiO_2 could be observed. Both the XRD spectrum of TiO_2 supported Pt and TiO_2 are identical. The lack of any diffraction peak of Pt on the Pt-doped TiO_2 catalyst reveals that Pt is well dispersed and in smaller quantities. Sharp peaks for TiO_2 demonstrate the strong crystalline nature of the particles [45]. However, compared to TiO_2, slight peak broadening could be observed in the case of Pt-impregnated TiO_2. This might be due to the presence of Pt on the surface of TiO_2 NPs. The crystallite size of TiO_2 NPs, calculated using Scherrer's formula, is 10.132 nm, whereas, for the TiO_2 supported Pt catalyst, it increased to 13.43 nm. The increase of the average particle size of TiO_2 by doping with Pt might be due to the position and inclusion of Pt (IV) with Ti (III) in TiO_2 lattice. The smaller crystallite size of the NPs is confirmed by the presence of a large BET surface area (129 m^2/g). The surface characterisation of TiO_2 and Pt/TiO_2 was evaluated with Brunauer–Emmet–Teller (BET) analysis in Figure 5, and the outcomes are reported in Table 1. The specific surface area of TiO_2 NPs is calculated as 71 m^2 /g. Interestingly, with the Pt doping on TiO_2, an enhancement in the specific surface area could be noticed, which is in line with the earlier observation [46].

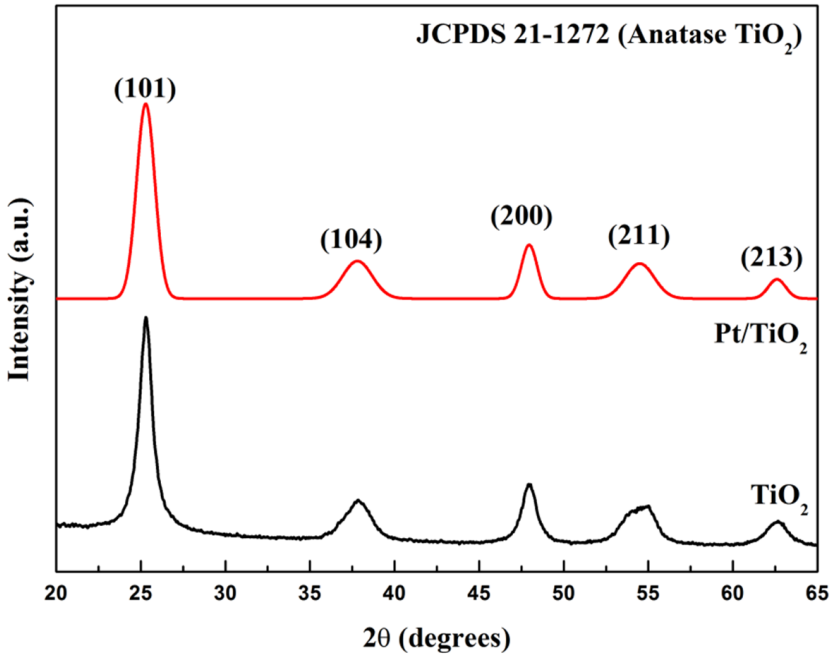

Figure 4. XRD spectrum of TiO_2 and TiO_2-supported Pt photocatalyst.

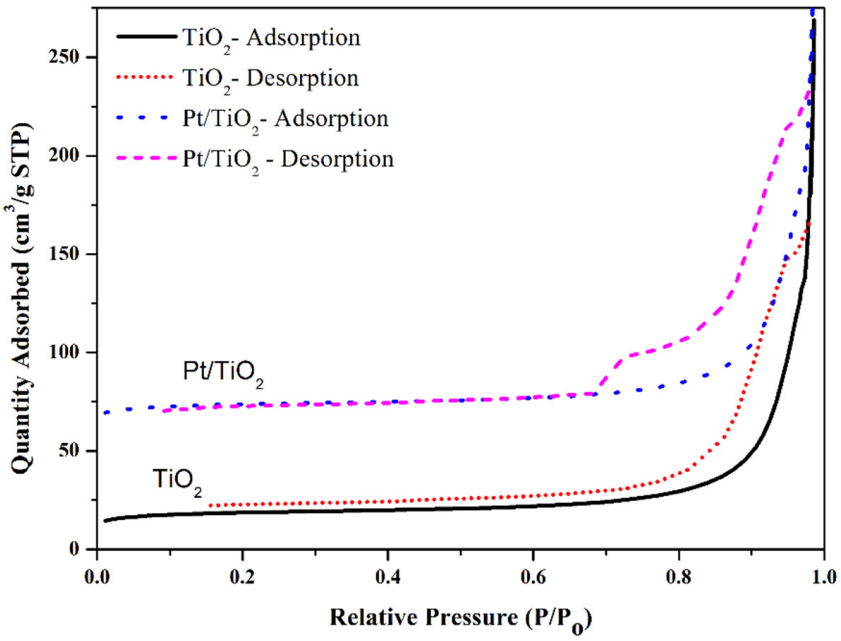

Figure 5. BET specific surface area of TiO_2 and Pt/TiO_2.

Table 1. Brunauer–Emmett–Teller (BET) analysis for the particle size and crystallite size: TiO_2, Pt/TiO_2.

Activated Carbon	Surface Area (m^2/g)	Pore Diameter (nm)	Pore Volume (cm^3/g)	Particle Size (TEM) (nm)	Crystallite Size Using Scherrer Equation (nm)
TiO_2	71	13.6	0.31	11	10.132
Pt/TiO_2	129	17.2	0.45	15	13.43

2.4.1. FE-SEM Analysis of TiO_2 and TiO_2 Supported Pt Catalyst

Field emission scanning electron microscopy (FE-SEM) gives the topographical information (10× to 300,000×). In the present synthesis, the particles were characterised with

a magnification of 50,000×, a scale of 1.0 µm, and 100,000× and 500 nm. They have been reported in Figures 6 and 7 for TiO_2 and Pt/TiO_2, respectively. FE-SEM analysis (Figure 4) shows that the TiO_2 particles are spherical, and Pt doping on the TiO_2 support did not change the morphology significantly (Figure 7). The morphology of Pt photocatalyst with TiO_2 support remains spherical.

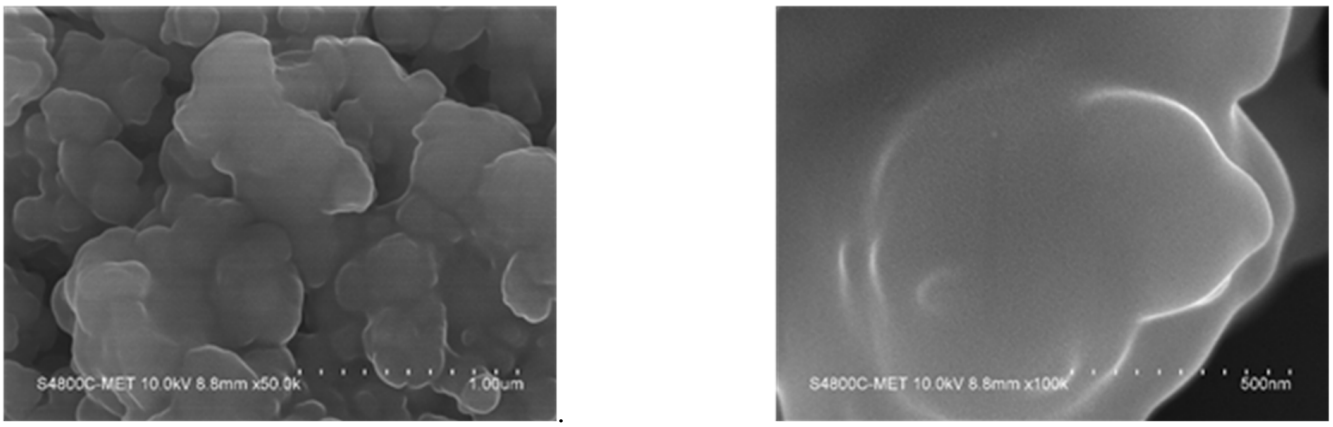

(**a**) (**b**)

Figure 6. FESEM images of TiO_2 at (**a**) 1 µm (**b**) 500 nm.

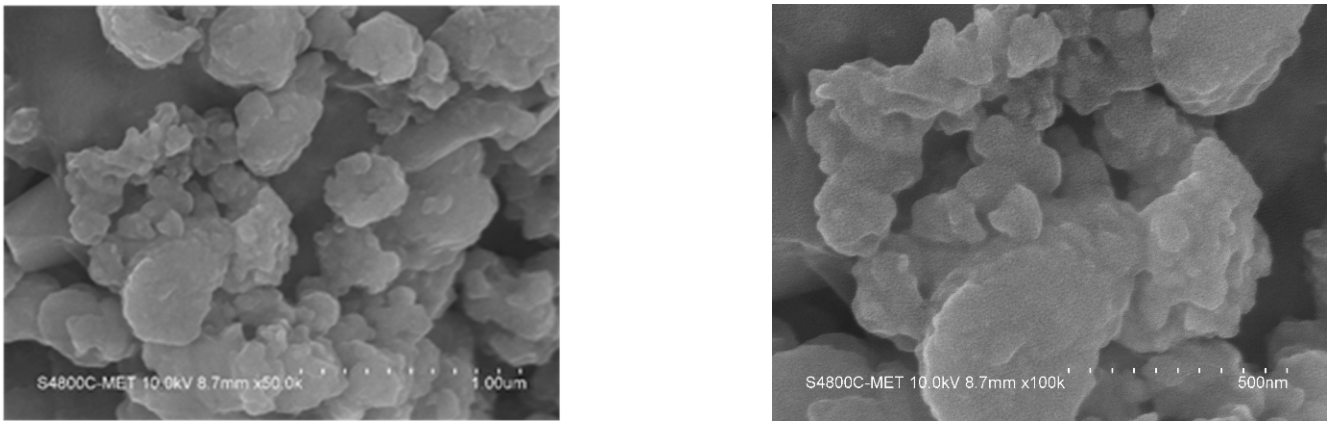

(**a**) (**b**)

Figure 7. FESEM images of Pt/TiO_2 at (**a**) 1 µm and (**b**) 500 nm.

2.4.2. TEM Analysis of TiO_2 and Pt/TiO_2

The microjets formed due to ultrasonic cavitation prevent the agglomeration of crystals and result in smaller crystal size and uniform particle size and shape [47]. The TEM images of the TiO_2 also confirmed the high degree of dispersion. The images (Figure 8a,b) clearly show that the Pt catalysts exhibit a uniform distribution over the TiO_2 support. The Pt/TiO_2 presents uniform dispersion of Pt on the TiO_2 surface. The mean particle size of pure TiO_2 was observed to be between 10 and 12 nm. The average particle size of Pt doped on TiO_2 NPs was found to be less than 15 nm confirming the nanoscale of supported metal catalyst for its photocatalytic effectiveness. The covalent radius of Pt is 1.30 Å, and for Pt^{2+} and Pt^{4+}, it is 0.80 and 0.65 Å, respectively. Titanium has an ionic radius of 0.68 Å in the Ti^{4+} state. Hence, Pt^{4+} ion is conveniently inserted into the TiO_2. Interestingly, the Pt^{4+} ions doping does not distort the photocatalyst [48].

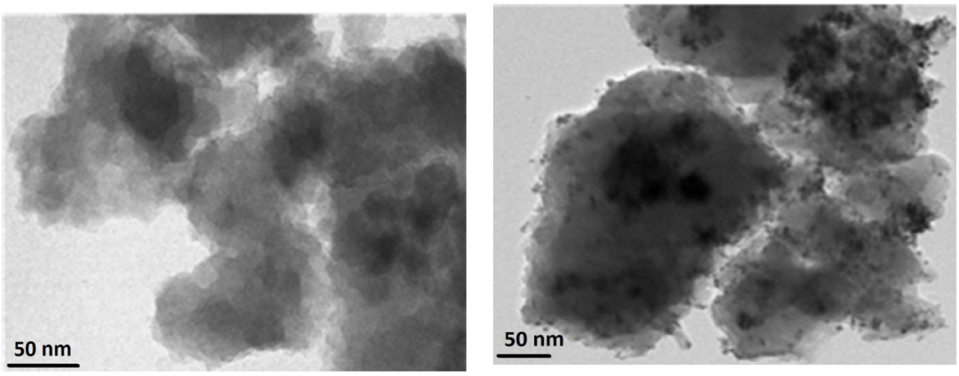

(**a**) (**b**)

Figure 8. TEM images (**a**) TiO_2 (**b**) TiO_2 supported Pt catalyst synthesised using acoustic cavitation.

2.5. Energy Dispersive X-Ray Analysis (EDX) (Pt/TiO$_2$)

Figure 9 depicts the EDX analysis for the TiO_2-supported Pt catalyst obtained using ultrasound. The strong peaks of titanium (41.28 wt%) and oxygen (55.51 wt%) in the spectra indicate that the concentration of support (TiO_2) is higher compared with Pt catalyst (3.21 wt%), as Pt is an expensive catalyst, and its lower percentage and good dispersion on the support is expected. The chemical composition of Pt/TiO_2 from the EDX analysis is shown in Table 2.

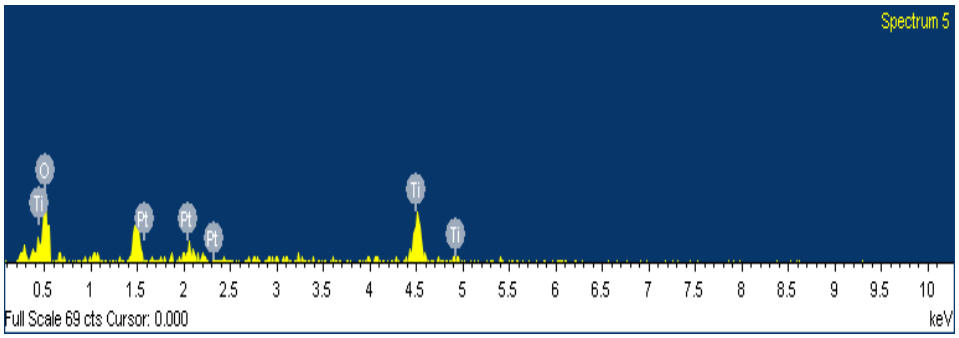

Figure 9. Energy-dispersive X-ray analysis of Pt/TiO_2 photocatalyst.

Table 2. Chemical composition of Pt/TiO_2 determined from EDX analysis.

Elements	Wt%	Atomic %
O	73.52	90.21
Ti	23.03	9.44
Pt	2.45	0.35

3. Materials and Methods

3.1. Materials

Titanium tetraisopropoxide (TTIP) (97%) was obtained from Spectrochem Pvt. Ltd. Mumbai, India. Sodium hydroxide (NaOH, 97%), methanol (HPLC grade), and acetone were obtained from Molychem Ltd., Mumbai, India. Potassium hexachloroplatinate (K_2PtCl_6) and sodium borohydride ($NaBH_4$, 98%) were procured from Sainergy fuel cell Pvt. Ltd. Chennai, India.

3.2. Synthesis of TiO$_2$ as the Support: Ultrasound Approach

TiO_2 NPs were synthesised using an ultrasound approach. To initiate the reaction, TTIP (10 mL) was mixed with acetone and methanol (2 mL each) in a 250 mL beaker and subjected to sonication. After initial mixing of TTIP, methanol, and acetone, dropwise

addition of 50 mL NaOH was initiated in the presence of ultrasound. The sonicator was operated in batch mode (2 s on and 1 s off) and was initially carried out for 30 min and then continued for another 15 min. The extended 15 min sonication was performed to ensure 100% conversion of TTIP. The formed white precipitate was filtered, dried, and calcination was carried out at 500 °C for 4 h. Earlier reports indicate that the calcination of TiO_2 NPs between 600 °C and 850 °C lead to either brookite, anatase, or rutile phase [49].

3.3. Synthesis of TiO_2 Supported Pt Catalyst

For the synthesis of TiO_2-supported Pt photocatalyst, TiO_2 support was obtained, as indicated in the previous section. For the doping of Pt catalyst, 70 mL polyvinyl propylene (PVP) (beaker A) dopant solution was prepared by dissolving PVP (10 mL) in Milli-Q water (70 mL). From the prepared PVP solution, 10 mL was taken in another beaker (beaker B), to which 0.5 g potassium hexachloroplatinate (K_2PtCl_6) and 0.75 g TiO_2 was dissolved. The solution in beaker B was kept under stirring for 6–8 h for proper dispersion. The remaining 60 mL PVP solution was taken in another beaker (beaker C), to which 0.037 g sodium borohydride ($NaBH_4$) reducing agent was added. The solution in beaker B and beaker C was mixed and sonicated using an ultrasound probe (Dakshin ultrasonic probe sonicator, frequency 22 kHz, with the total power supply of 130 W) for 2 h to ensure the completion of the reaction. Figure 10a shows the synthesis pathway, whereas Figure 10b,c shows the reaction mixture before and after sonication, respectively. The reaction completion was confirmed by the changes in the solution colour (black). The synthesised particles were separated from the solution by centrifugation (9000 rpm and 10 °C for 12 min) and were dried at 150 °C.

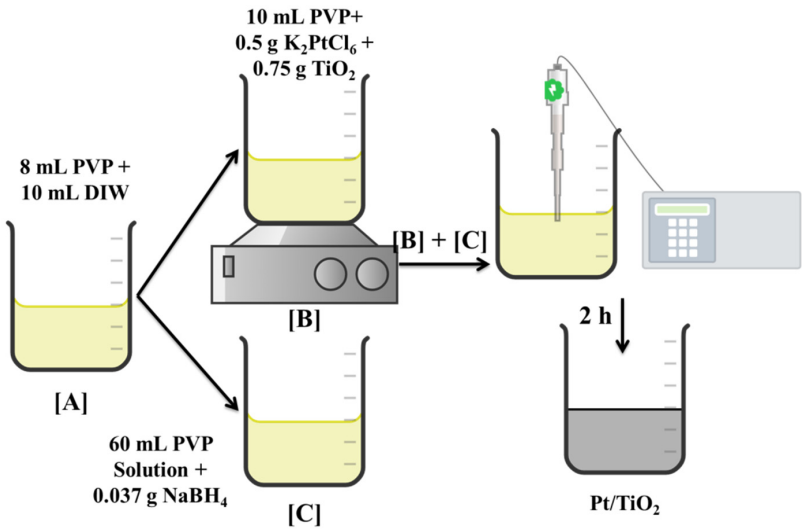

(**a**)

(**b**) (**c**)

Figure 10. (**a**) Synthesis pathway (**b**) Mixture of Pt/TiO_2 (before reaction) (**c**) Mixture of Pt/TiO_2 (after reaction).

4. Characterisation

A UV-visible spectrometer (Analytik Jena, PECORD 210 PLUS) was employed to find the band gap energy of the synthesised TiO_2 and Pt/TiO_2 particles. The particle size analysis (PSA) of the synthesised support and photocatalyst was carried out using the dynamic light scattering method with Malvern Zetasizer (Nano S90 version 7.02). X-ray diffraction studies were performed to identify the phase and determine the crystallite size of the TiO_2 and Pt-doped TiO_2. Bruker D8 advanced X-ray diffractometer, operated in reflection mode, was used to record the XRD spectra with CuKα as the X-ray source with the wavelength of 0.154 nm. The spectra were recorded for 2θ between 10° and 90° with a step size of 0.019, and the corresponding intensity values were plotted against 2θ (degree). FE-SEM (TESCAN model Vega 3 LMU) was used primarily to study the surface morphology where the sample was spread over a substrate and analysed. The morphology and size of the synthesised TiO_2 support and TiO_2-supported Pt photocatalyst were evaluated using FEI-TechnaiTE-20 and JEOL JEM-2100F field emission transmission electron microscope operated at 200 kV. The surface characteristics of the support TiO_2 and TiO_2-supported Pt catalyst were evaluated through Brunauer–Emmett–Teller (BET) analysis. The nitrogen adsorption-desorption method was used to estimate the particle surface area, pore size and volume. The BET analysis was carried out using the NOVA 1200 (Quantachrome) instrument at 77.3 K. The samples were degassed under vacuum conditions at 353 K for 4 to 5 h to remove the adsorbed gases and moisture before the analysis.

5. Conclusions

In this study, a photoactive TiO_2 catalyst was synthesised with an ultrasound approach to improve the photocatalytic performance of TiO_2, and it was doped with a noble metal Pt. The impregnation helps to reduce the band gap and effective utilisation as a photocatalyst in the visible range. The synthesised TiO_2 and Pt impregnated TiO_2 photocatalyst exhibit a crystal size of less than 10 nm. The FE-SEM analysis showed that doping Pt onto titanium does not change the morphology. The uniform dispersion of a small quantity of Pt on the TiO_2 support was confirmed using TEM analysis and corroborated by EDX spectra which exhibits a less intense peak of Pt. The nanoscale synthesis is attributed to the intense shear effect arising from ultrasound cavitation. The enhancement in the surface properties of TiO_2 due to the addition of Pt was evaluated in terms of an increase in the surface area of the synthesised photocatalyst. Thus, the ultrasound approach can be considered greener and more energy-efficient for synthesising highly active photocatalysts.

Author Contributions: S.B.P.: contributed to the synthesis, experiments, analysis of data and writing the first draft of the manuscript. C.-M.H.: contributed to data analysis and revising the paper. B.P.: contributed to data interpretation and writing the paper. S.M.: contributed with TEM and BET analysis, writing and revising the paper. S.H.S.: conceived and designed the work and revising the manuscript. All authors have read and agreed to the published version of the manuscript.

Funding: Chao-Ming Huang thanks the funding support by the Ministry of Science and Technology (MOST 110-2637-E-168-002), Taiwan.

Conflicts of Interest: The authors declare no conflict of interest.

References

1. Schneider, J.; Matsuoka, M.; Takeuchi, M.; Zhang, J.; Horiuchi, Y.; Anpo, M.; Bahnemann, D.W. Understanding TiO_2 Photocatalysis: Mechanisms and Materials. *Chem. Rev.* **2014**, *114*, 9919–9986. [CrossRef] [PubMed]
2. Yin, S.; Liu, B.; Zhang, P.; Morikawa, T.; Yamanaka, K.I.; Sato, T. Photocatalytic oxidation of NOx under visible led light irradiation over nitrogen-doped titania particles with iron or platinum loading. *J. Phys. Chem. C* **2008**, *112*, 12425–12431. [CrossRef]
3. Sakthivel, S.; Neppolian, B.; Arabindoo, B.; Palanichamy, M.; Murugesan, V. TiO_2 catalysed photodegradation of leather dye, Acid Green 16. *J. Sci. Ind. Res.* **2000**, *59*, 556–562.
4. Zaleska, A. Doped-TiO_2: A Review. *Recent Pat. Eng.* **2008**, *2*, 157–164. [CrossRef]
5. Landge, V.K.; Sonawane, S.H.; Chaudhari, R.V.; Babu, G.U.B. Selective Oxidation of Glycerol: A Biomass-Derived Feedstock Using the Pt-Cu Janus Catalyst for Value-Added Products. *Ind. Eng. Chem. Res.* **2020**, *60*, 185–195. [CrossRef]

6. Lü, X.; Mou, X.; Wu, J.; Zhang, D.; Zhang, L.; Huang, F.; Xu, F.; Huang, S. Improved-Performance Dye-Sensitized solar cells using Nb-Doped TiO_2 electrodes: Efficient electron Injection and transfer. *Adv. Funct. Mater.* **2010**, *20*, 509–515. [CrossRef]
7. Mohamed, N.M.; Bashiri, R.; Chong, F.K.; Sufian, S.; Kakooei, S. Photoelectrochemical behaviour of bimetallic Cu-Ni and monometallic Cu, Ni doped TiO_2 for hydrogen production. *Int. J. Hydrog. Energy* **2015**, *40*, 14031–14038. [CrossRef]
8. Chen, L.; He, S.; He, B.Y.; Wang, T.J.; Su, C.L.; Zhang, C.; Jin, Y. Synthesis of iron-doped titanium oxide nano adsorbent and its adsorption characteristics for fluoride in drinking water. *Ind. Eng. Chem. Res.* **2012**, *51*, 13150–13156. [CrossRef]
9. Cheng, T.; Gao, H.; Liu, G.; Pu, Z.; Wang, S.; Yi, Z.; Wu, X.; Yang, H. Preparation of Core-Shell Heterojunction Photocatalysts by Coating CdS Nanoparticles onto Bi4Ti3O12 Hierarchical Microspheres and Their Photocatalytic Removal of Organic Pollutants and Cr(VI) Ions. *Colloids Surf. A Physicochem. Eng. Asp.* **2022**, *633*, 127918. [CrossRef]
10. Khalid, N.R.; Majid, A.; Tahir, M.B.; Niaz, N.A.; Khalid, S. Carbonaceous-TiO_2 nanomaterials for photocatalytic degradation of pollutants: A review. *Ceram. Int.* **2017**, *43*, 14552–14571. [CrossRef]
11. Fernández-Rodríguez, C.; Doña-Rodríguez, J.M.; González-Díaz, O.; Seck, I.; Zerbani, D.; Portillo, D.; Perez-Peña, J. Synthesis of highly photoactive TiO_2 and Pt/TiO_2 nanocatalysts for substrate-specific photocatalytic applications. *Appl. Catal. B Environ.* **2012**, *125*, 383–389. [CrossRef]
12. Sadanandam, G.; Lalitha, K.; Kumari, V.D.; Shankar, M.V.; Subrahmanyam, M. Cobalt doped TiO_2: A stable and efficient photocatalyst for continuous hydrogen production from glycerol: Water mixtures under solar light irradiation. *Int. J. Hydrog. Energy* **2013**, *38*, 9655–9664. [CrossRef]
13. Bagheri, S.; Muhd Julkapli, N.; Bee Abd Hamid, S. Titanium dioxide as a catalyst support in heterogeneous catalysis. *Sci. World J.* **2014**, *2014*, 1–21. [CrossRef]
14. Rao, T.N.; Babji, P.; Ahmad, N.; Khan, R.A.; Hassan, I.; Shahzad, S.A.; Husain, F.M. Green synthesis and structural classification of Acacia nilotica mediated-silver doped titanium oxide (Ag/TiO_2) spherical nanoparticles: Assessment of its antimicrobial and anticancer activity. *Saudi J. Biol. Sci.* **2019**, *26*, 1385–1391. [CrossRef]
15. Ould-Chikh, S.; Proux, O.; Afanasiev, P.; Khrouz, L.; Hedhili, M.N.; Anjum, D.H.; Harb, M.; Geantet, C.; Basset, J.M.; Puzenat, E. Photocatalysis with chromium-doped TiO_2: Bulk and surface doping. *ChemSusChem* **2014**, *7*, 1361–1371. [CrossRef]
16. Wang, S.; Bai, L.N.; Sun, H.M.; Jiang, Q.; Lian, J.S. Structure and photocatalytic property of Mo-doped TiO_2 nanoparticles. *Powder Technol.* **2013**, *244*, 9–15. [CrossRef]
17. Wu, J.C.S.; Chen, C.H. A visible-light response vanadium-doped titania nanocatalyst by sol-gel method. *J. Photochem. Photobiol. A Chem.* **2004**, *163*, 509–515. [CrossRef]
18. Gupta, K.; Singh, R.P.; Pandey, A.; Pandey, A. Photocatalytic antibacterial performance of TiO_2 and Ag-doped TiO_2 against *S. aureus*. *P. aeruginosa* and *E. coli*. *Beilstein J. Nanotechnol.* **2013**, *4*, 345–351. [CrossRef]
19. Singh, S.A.; Madras, G. Sonochemical synthesis of Pt, Ru doped TiO_2 for methane reforming. *Appl. Catal. A Gen.* **2016**, *518*, 102–114. [CrossRef]
20. Ihnatiuk, D.; Tossi, C.; Tittonen, I.; Linnik, O. Effect of synthesis conditions of nitrogen and platinum co-doped titania films on the photocatalytic performance under simulated solar light. *Catalysts* **2020**, *10*, 1074. [CrossRef]
21. Grabowska, E.; Remita, H.; Zaleska, A. Photocatalytic activity of TiO_2 loaded with metal clusters. *Physicochem. Probl. Miner. Process.* **2010**, *45*, 29–38.
22. Li, Y.; Li, M.; Xu, P.; Tang, S.; Liu, C. Efficient Photocatalytic Degradation of Acid Orange 7 over N-Doped Ordered Mesoporous Titania on Carbon Fibers under Visible-Light Irradiation Based on Three Synergistic Effects. *Appl. Catal. A Gen.* **2016**, *524*, 163–172. [CrossRef]
23. Mohamed, R.M.; Baeissa, E.S. Mordenite encapsulated with Pt-TiO_2: Characterisation and applications for photocatalytic degradation of direct blue dye. *J. Alloys Compd.* **2013**, *558*, 68–72. [CrossRef]
24. Xiong, S.; Yin, Z.; Zhou, Y.; Peng, X.; Yan, W.; Liu, Z.; Zhang, X. The Dual-Frequency (20/40 KHz) Ultrasound Assisted Photocatalysis with the Active Carbon Fiber-Loaded Fe^{3+}-TiO_2 as Photocatalyst for Degradation of Organic Dye. *Bull. Korean Chem. Soc.* **2013**, *34*, 3039–3045. [CrossRef]
25. Devipriya, S.P.; Yesodharan, S.; Yesodharan, E.P. Solar photocatalytic removal of chemical and bacterial pollutants from water using Pt/TiO_2-coated ceramic tiles. *Int. J. Photoenergy* **2012**, *2012*, 1–8. [CrossRef]
26. Kim, S.; Hwang, S.J.; Choi, W. Visible light active platinum-ion-doped TiO_2 photocatalyst. *J. Phys. Chem. B* **2005**, *109*, 24260–24267. [CrossRef] [PubMed]
27. Lin, X.; Li, M.; Li, Y.; Chen, W. Enhancement of the Catalytic Activity of Ordered Mesoporous TiO_2 by Using Carbon Fiber Support and Appropriate Evaluation of Synergy between Surface Adsorption and Photocatalysis by Langmuir-Hinshelwood (L-H) Integration Equation. *RSC Adv.* **2015**, *5*, 105227–105238. [CrossRef]
28. Rodríguez-Martínez, C.; García-Domínguez, Á.E.; Guerrero-Robles, F.; Saavedra-Díaz, R.O.; Torres-Torres, G.; Felipe, C.; Ojeda-López, R.; Silahua-Pavón, A.; Cervantes-Uribe, A. Synthesis of supported metal nanoparticles (Au/TiO_2) by the suspension impregnation method. *J. Compos. Sci.* **2020**, *4*, 89. [CrossRef]
29. Abbas, M.M.; Rasheed, M. Solid State Reaction Synthesis and Characterization of Cu doped TiO_2 Nanomaterials. *J. Phys. Conf. Ser.* **2021**, *1795*, 1–9. [CrossRef]
30. Tang, N.; Li, Y.; Chen, F.; Han, Z. In Situ Fabrication of a Direct Z-Scheme Photocatalyst by Immobilising CdS Quantum Dots in the Channels of Graphene-Hybridized and Supported Mesoporous Titanium Nanocrystals for High Photocatalytic Performance under Visible Light. *RSC Adv.* **2018**, *8*, 42233–42245. [CrossRef]

31. Fan, C.; Chen, C.; Wang, J.; Fu, X.; Ren, Z.; Qian, G.; Wang, Z. Black Hydroxylated Titanium Dioxide Prepared via Ultrasonication with Enhanced Photocatalytic Activity. *Sci. Rep.* **2015**, *5*, 1–10. [CrossRef]
32. Teoh, W.Y.; Mädler, L.; Beydoun, D.; Pratsinis, S.E.; Amal, R. Direct (one-step) synthesis of TiO_2 and Pt/TiO_2 nanoparticles for photocatalytic mineralisation of sucrose. *Chem. Eng. Sci.* **2005**, *60*, 5852–5861. [CrossRef]
33. Shanmugam, S.; Gedanken, A. Synthesis and electrochemical oxygen reduction of platinum nanoparticles supported on mesoporous TiO_2. *J. Phys. Chem. C* **2009**, *113*, 18707–18712. [CrossRef]
34. Neppolian, B.; Bruno, A.; Bianchi, C.L.; Ashokkumar, M. Graphene oxide based Pt-TiO_2 photocatalyst: Ultrasound assisted synthesis, characterisation and catalytic efficiency. *Ultrason. Sonochem.* **2012**, *19*, 9–15. [CrossRef] [PubMed]
35. Bedolla-Valdez, Z.I.; Verde-Gómez, Y.; Valenzuela-Muñiz, A.M.; Gochi-Ponce, Y.; Oropeza-Guzmán, M.T.; Berhault, G.; Alonso-Núñez, G. Sonochemical synthesis and characterization of Pt/CNT, Pt/TiO_2, and Pt/CNT/TiO_2 electrocatalysts for methanol electro-oxidation. *Electrochim. Acta* **2015**, *186*, 76–84. [CrossRef]
36. Abdulrazzak, F.H.; Hussein, F.H.; Alkaim, A.F.; Ivanova, I.; Emeline, A.V.; Bahnemann, D.W. Sonochemical/hydration-dehydration synthesis of Pt-TiO_2 NPs/decorated carbon nanotubes with enhanced photocatalytic hydrogen production activity. *Photochem. Photobiol. Sci.* **2016**, *15*, 1347–1357. [CrossRef] [PubMed]
37. Driessen, M.D.; Grassian, V.H. Photooxidation of Trichloroethylene on Pt/TiO_2. *J. Phys. Chem. B.* **1997**, *102*, 1418–1423. [CrossRef]
38. Zhu, Z.; Wu, R.J. The Degradation of Formaldehyde Using a Pt@TiO_2 Nanoparticles in Presence of Visible Light Irradiation at Room Temperature. *J. Taiwan Inst. Chem. Eng.* **2015**, *50*, 276–281. [CrossRef]
39. Pinedo-Escobar, J.A.; Fan, J.; Moctezuma, E.; Gomez-Solís, C.; Martinez, C.J.C.; Gracia-Espino, E. Nanoparticulate double-heterojunction photocatalysts comprising TiO_2 (Anatase)/WO_3/TiO_2 (Rutile)with enhanced photocatalytic activity toward the degradation of methyl orange under near-ultraviolet and visible light. *ACS Omega* **2021**, *6*, 11840–11848. [CrossRef]
40. Zhao, Z.J.; Hwang, S.H.; Jeon, S.; Hwang, B.; Jung, J.Y.; Lee, J.; Park, S.H.; Jeong, J.H. Three-Dimensional Plasmonic Ag/TiO_2 Nanocomposite Architectures on Flexible Substrates for Visible-Light Photocatalytic Activity. *Sci. Rep.* **2017**, *7*, 1–11. [CrossRef]
41. Kim, H.; Choi, Y.; Kanuka, N.; Kinoshita, H.; Nishiyama, T.; Usami, T. Preparation of Pt-loaded TiO_2 nanofibers by electrospinning and their application for WGS reactions. *Appl. Catal. A Gen.* **2009**, *352*, 265–270. [CrossRef]
42. Boccuzzi, F.; Chiorino, A.; Manzoli, M.; Andreeva, D.; Tabakova, T.; Ilieva, L.; Iadakiev, V. Gold, silver and copper catalysts supported on TiO_2 for pure hydrogen production. *Catal. Today* **2002**, *75*, 169–175. [CrossRef]
43. Balachandramohan, J.; Sivasankar, T.; Sivakumar, M. Facile sonochemical synthesis of Ag_2O-guar gum nanocomposite as a visible light photocatalyst for the organic transformation reactions. *J. Hazard. Mater.* **2020**, *385*, 121621. [CrossRef] [PubMed]
44. Sivakumar, M.; Towata, A.; Yasui, K.; Tuziuti, T.; Kozuka, T.; Tsujimoto, M.; Zhong, Z.; Iida, Y. Fabrication of nanosized Pt on rutile TiO_2 using a standing wave sonochemical reactor (SWSR)—Observation of an enhanced catalytic oxidation of CO. *Ultrason. Sonochem.* **2010**, *17*, 213–218. [CrossRef]
45. Ahmed, L.M.; Ivanova, I.; Hussein, F.H.; Bahnemann, D.W. Role of Platinum Deposited on TiO_2 in Photocatalytic Methanol Oxidation and Dehydrogenation Reactions. *Int. J. Photoenergy* **2014**, *2014*, 1–9. [CrossRef]
46. Abdennouri, M.; Elhalil, A.; Farnane, M.; Tounsadi, H.; Mahjoubi, F.Z.; Elmoubarki, R.; Sadiq, M.; Khamar, L.; Galadi, A.; Baâlala, M.; et al. Photocatalytic degradation of 2,4-D and 2,4-DP herbicides on Pt/TiO_2 nanoparticles. *J. Saudi Chem. Soc.* **2015**, *19*, 485–493. [CrossRef]
47. Potdar, S.B.; Praveen, B.V.S.; Sonawane, S.H. Sonochemical approach for synthesis of zinc oxide-poly methyl methacrylate hybrid nanoparticles and its application in corrosion inhibition. *Ultrason. Sonochem.* **2020**, *68*, 1–7. [CrossRef]
48. Hong, G.B.; Ma, C.M. Photocatalytic degradation of indoor air pollutants by Pt-TiO_2. *J. Nanomater.* **2012**, *2012*, 88–92. [CrossRef]
49. Bethi, B.; Sonawane, S.H.; Rohit, G.S.; Holkar, C.R.; Pinjari, D.V.; Bhanvase, B.A.; Pandit, A.B. Investigation of TiO_2 photocatalyst performance for decolorisation in the presence of hydrodynamic cavitation as hybrid AOP. *Ultrason. Sonochem.* **2016**, *28*, 150–160. [CrossRef]